# Siderophore-controlled iron assimilation in the enterobacterium Erwinia chrysanthemi : evidence for the involvement of bacterioferritin and the Suf iron-sulfur cluster assembly machinery

Dominique Expert, Aïda Boughammoura, Thierry T. Franza

THE JOURNAL OF BIOLOGICAL CHEMISTRY VOL. 283, NO. 52, pp. 36564–36572, December 26, 2008


# Siderophore-controlled Iron Assimilation in the Enterobacterium *Erwinia chrysanthemi*

## *EVIDENCE FOR THE INVOLVEMENT OF BACTERIOFERRITIN AND THE Suf IRON-SULFUR CLUSTER ASSEMBLY MACHINERY**[S]

Received for publication, October 7, 2008, and in revised form, November 6, 2008 Published, JBC Papers in Press, November 6, 2008, DOI 10.1074/jbc.M807749200

**Dominique Expert**[1], **Aïda Boughammoura**[2], **and Thierry Franza**

*From the Laboratoire Interactions Plantes-Pathogènes, Unité Mixte de Recherche 217, Institut National de la Recherche Agronomique, AgroParisTech, Université Paris 6, 75005 Paris, France*

**The intracellular fate of iron acquired by bacteria during siderophore-mediated assimilation is poorly understood. We investigated this question in the pathogenic enterobacterium *Erwinia chrysanthemi*. This bacterium produces two siderophores, chrysobactin and achromobactin, during plant infection. We analyzed the distribution of iron into cytosolic proteins in bacterial cells supplied with $^{59}$Fe-chrysobactin using native gel electrophoresis. A parental strain and mutants deficient in bacterioferritin (*bfr*), miniferritin (*dps*), ferritin (*ftnA*), bacterioferredoxin (*bfd*), or iron-sulfur cluster assembly machinery (*sufABCDSE*) were studied. In the parental strain, we observed two rapidly $^{59}$Fe-labeled protein signals identified as bacterioferritin and an iron pool associated to the protein chain-elongation process. In the presence of increased $^{59}$Fe-chrysobactin concentrations, we detected mini-ferritin-bound iron. Iron incorporation into bacterioferritin was severely reduced in nonpolar *sufA*, *sufB*, *sufD*, *sufS*, *and sufE* mutants but not in a *sufC* background. Iron recycling from bacterioferritin did not occur in *bfd* and *sufC* mutants. Iron depletion caused a loss of aconitase activity, whereas ferric chrysobactin supplementation stimulated the production of active aconitase in parental cells and in *bfr* and *bfd* mutants. Aconitase activity in *sufA*, *sufB*, *sufD*, *sufS*, and *sufE* mutant strains was 10 times lower than that in parental cells. In the *sufC* mutant, it was twice as low as that in the parental strain. Defects observed in the mutants were not caused by altered ferric chrysobactin transport. Our data demonstrate a functional link between bacterioferritin, bacterioferredoxin, and the Suf protein machinery resulting in optimal bacterial growth and a balanced distribution of iron between essential metalloproteins.**

Iron is necessary for most forms of life, being required for the catalytic activity of essential proteins mediating electron transfer and redox reactions. The importance of this metal relies on its electronic structure, which can undergo changes through several oxidation states differing by one electron. The ferric form of iron predominates in aerobic environments, but its bioavailability is severely compromised by its poor solubility (1). Ferrous iron is present at significant levels in the cell but can be toxic as a consequence of its participation in "Fenton-type" redox chemistry (2, 3). Thus, iron acquisition, utilization, and storage are subject to different levels of homeostatic regulation.

Microorganisms have developed powerful iron acquisition systems based on production of siderophores, which are selective ferric ion chelators secreted in response to iron deficiency (4). Once loaded with iron, the siderophore is specifically imported into the cell. This requires active transport which, in Gram-negative bacteria, is achieved by a TonB-dependent outer membrane receptor and a permease belonging to the ABC transporter family (5). Regulation of siderophore production and uptake involves the metalloprotein Fur[3] or functional analogs, acting as transcriptional repressors of iron-responsive genes (6). Although major advances have improved understanding of the processes involved in ferric siderophore uptake, there is still little information on the intracellular fate of iron, once released from its ligand. Enzymatic degradation of the ferric siderophore complex and/or enzymatic reduction to the ferrous state are effective mechanisms for iron removal (7). It remains to be determined how the cell prioritizes its intracellular iron utilization so that iron-containing proteins preferentially receive iron, at the same time avoiding toxic side reactions. Of the various classes of iron-containing proteins, iron-sulfur proteins and ferritins are of particular interest.

Biosynthesis of iron-sulfur proteins involves complex protein machineries that build iron-sulfur clusters from cytosolic iron and sulfur sources and transfer them to their cognate protein acceptors. Studies in various bacterial species, including *Escherichia coli*, *Erwinia chrysanthemi*, and cyanobacteria have led to the identification of the Isc and Suf machinery, which have homologs in eukaryotes (8–10). The mechanisms by which Isc or Suf proteins work together have been an area of intense investigations (11, 12). The proteins encoded by the *isc* operon appear to mediate a general pathway for the assembly of

* This work was supported by the Institut National de la Recherche Agronomique. The costs of publication of this article were defrayed in part by the payment of page charges. This article must therefore be hereby marked "*advertisement*" in accordance with 18 U.S.C. Section 1734 solely to indicate this fact.

[S] The on-line version of this article (available at http://www.jbc.org) contains supplemental Tables S1–S3 and Fig. S1.

[1] Researcher from the Centre National de la Recherche Scientifique (CNRS). To whom correspondence should be addressed: 16 rue Claude Bernard, 75005 Paris, France. Fax: 33-01-44-08-16-31; E-mail: expert@agroparistech.fr.

[2] Supported by a doctoral fellowship from the Ministère de l'Education Nationale, de l'Enseignement Supérieur et de la Recherche. Present address: Laboratoire de Biotechnologies et de Génétique Appliquée, Ecole Normale Supérieure de Cachan, 61 Ave. du Président Wilson, 94235 Cachan, France.

[3] The abbreviations used are: Fur, ferric uptake regulation; Isc, iron-sulfur cluster; Suf, sulfur utilization factor; Ftn, ferritin; Bfr, bacterioferritin; Dps, DNA protein from starved cells; Bfd, bacterioferredoxin; FMP, fast migrating proteins.

a variety of iron-sulfur proteins, whereas those encoded by the *suf* operon play a role in iron-sulfur cluster biosynthesis under conditions of iron deficiency or oxidative stress (13–15). The iron donation step for cluster assembly *in vivo* is unknown (16, 17). In eukaryotes, the mitochondrial frataxin protein has been proposed to act as an iron donor for assembly of iron-sulfur clusters (18, 19) and a similar function was assigned to the bacterial homolog CyaY for the Isc machinery, although this still needs to be confirmed (16). The ability of the Suf pathway to function when iron is limiting suggests not only that Suf is involved in iron-sulfur cluster assembly but also that Suf may act as an iron trap.

Ferritins are iron storage proteins that sequester iron in a nonreactive form, protecting the cell from iron-induced toxicity (20, 21). In bacteria, these proteins are present in the same compartment as other iron-requiring proteins falling into three categories: heme-free ferritins (Ftn), found in prokaryotes and eukaryotes; heme-containing bacterioferritins (Bfr), found only in bacteria; and Dps proteins, also called mini-ferritins, present only in prokaryotes (22, 23). Ferritins and bacterioferritins are composed of 24 identical subunits, and Dps proteins contain 12 identical subunits. These subunits assemble to make a spherical protein shell surrounding a central cavity able to hold up to between 2,000 and 3,000 ferric iron atoms for ferritins and 500 atoms for mini-ferritins (21, 24). Ferritins have a binuclear di-iron center constituting the ferroxidase center, which is involved in the oxidation of the ferrous iron (25–28). Ferritins can act as acceptors and donors of ferrous ions, but their precise contribution in bacterial iron metabolism is not well understood.

An appropriate system physiologically relevant and representative of the bacterial world is needed to address these unresolved issues. We have developed *E. chrysanthemi* (*Dickeya dadantii*) as a model plant pathogen to investigate the role of iron during infection (29). The genome sequence of this bacterium is available and like many other bacterial species pathogenic to mammals, *E. chrysanthemi* requires powerful iron transport routes to obtain iron from host tissues. Notably, this bacterium produces two siderophores, chrysobactin and achromobactin, which are important for its virulence (30). Successful infection also requires a functional Suf system (31). The *E. chrysanthemi* FtnA ferritin and Bfr bacterioferritin have different roles *in vivo*. Like in *E. coli*, expression of the cognate *ftnA* gene is positively controlled by iron and the Fur repressor through a mechanism involving the small antisense RNA RyhB (32). The *E. chrysanthemi bfr* gene is clustered into an operon with the *bfd* gene that encodes a 64-amino acid peptide (Bfd). This peptide shows 70% of sequence identity with the bacterioferritin-associated [2Fe-2S] ferredoxin from *E. coli* K-12 (33, 34). The operon is expressed at a basal level and up-regulated at the stationary phase of growth by the sigma S factor (32). The *E. chrysanthemi* genome sequence also revealed the existence of a gene (*dps*) encoding a putative mini-ferritin (Dps).

In this study, we investigated the distribution of iron bound to cytosolic proteins from *E. chrysanthemi* mutant cells defective in siderophore biosynthesis, supplied with $^{59}$Fe via chrysobactin. The addition of iron stimulates growth and leads to global metabolic recovery in iron-deprived cells. We compared mutants deficient in bacterioferritin, bacterioferredoxin, ferritin, mini-ferritin, various Suf proteins, and Fur protein. We demonstrated a functional link between Bfr, Bfd, and the Suf protein machinery, which results in the balanced distribution of iron between essential proteins.

## EXPERIMENTAL PROCEDURES

*Bacterial Strains, Plasmids, and Microbiological Techniques*—The bacterial strains and plasmids used are described in supplemental Table S1. The *cbsE-1*, *cbsC-1*, *acsA-37*, *acsF*::Ω and *dps*::Ω mutations were introduced into the appropriate *bfr*, *ftnA*, *suf*, and *fur* deficient mutants by transduction using phage φEC2 as described previously (35). The rich media used were L broth and L agar (36). Tris medium was used as a low iron minimal medium (37). Glassware for Tris medium was treated as described previously (37). For iron-replete conditions, Tris medium was supplemented with ferric chrysobactin at the concentrations indicated. Ferric chrysobactin was prepared by adding $FeCl_3$ to chrysobactin in 0.1 M Tris, pH 7.5, at a ligand/iron ratio of 3:1. Glucose (2 g/liter) was used as carbon source. The antibacterial agents and chemicals were used as reported previously (35, 37) unless otherwise specified.

*Construction of the dps and bfd Deficient Mutants and General DNA Methods*—A genomic fragment from the *dps* locus was amplified by PCR with the primers 5′ sense dps1s (5′-attatcgcctcgctggga-3′) and 3′ reverse dps1r (5′-catcaaaacgtcctcctc-3′) and cloned using the pGEM-T Easy vector. This fragment was then subcloned into the pBC plasmid using appropriate restriction enzymes to introduce a unique EcoRV restriction site into the *dps* gene. The Ω-*Spec* interposon from pHP45Ω hydrolyzed with SmaI was inserted into the EcoRV site to obtain plasmid pAB12 (38, 39). To introduce a nonpolar mutation in the *bfd* gene, the *apha-3* cassette, obtained by SmaI digestion of pUC18K, was inserted into the T4 Polymerase blunted NsiI site of pAB3 (40). Plasmid transformation and marker exchange recombination with the chromosome were performed as described previously (37). Correct recombination was confirmed by PCR and Southern blot hybridization experiments. For construction of plasmid pAB14, a genomic fragment from the *bfd-bfr* encoding locus was amplified by PCR with the primers sense bfr1s (5′-ggtcgtgtagagcggca-3′) and reverse bfdr (5′-gtagaagcggtcaacacagag-3′) and inserted into the pGEM-T Easy vector. This fragment was subcloned into the ApaI and SpeI sites of the pBC plasmid. DNA manipulation techniques (chromosomal DNA isolation, cloning, and electrophoresis) were described previously (35). Plasmids were extracted using the QIAprep spin miniprep kit (Qiagen). All of the cloning experiments were performed in the DH5α strain of *E. coli*. PCR was performed in a DNA thermocycler (Hybaid PCR Express System) with denaturation at 94 °C for 60 s, annealing at 52 °C for 75 s, an extension at 72 °C for 90 s, and a final extension at 72 °C for 10 min. PCR products were cloned using the plasmid pGEM-T Easy, according to the manufacturer's instructions. Nucleotide sequences of PCR products and plasmids were obtained from Genome Express.

*In Vivo Labeling of Bacterial Cultures, Preparation of Whole Cell Extracts, and Analysis of Protein-bound $^{59}$Fe Iron*—An overnight culture in L broth of the strain to be studied was

diluted 1:40 in 5 ml of Tris medium supplemented with glucose placed in a 50-ml Erlenmeyer flask and incubated with shaking until $A_{600\ nm} = 0.4$ was reached. Iron labeling was started by adding a ferric chrysobactin complex solution prepared with $^{59}FeCl_3$ (3–20 mCi/mg iron in 0.5 M HCl; GE Healthcare). Samples (1 ml) were taken at the indicated times. Excess unlabeled ferric chrysobactin was added to each sample. Bacterial cells were spun down in a microcentrifuge, at 7000 RPM at 4 °C. The cells were washed in a solution containing 50 mM potassium phosphate, pH 7.8, 0.1 mM EDTA, and 10 mM $MgCl_2$ and harvested by centrifugation. The bacterial pellets were resuspended in 20–40 μl of the same solution with DNase I and lysozyme added at final concentrations of 0.1 and 0.2 mg/ml, respectively, and incubated for 30 min at 4 °C. The cells were lysed by six freeze/thaw cycles. The extracts were centrifuged at 15,000 × g for 5 min, and supernatant fluids were kept at −20 °C. To analyze the fate of iron during bacterial growth, labeled cells were centrifuged at 3000 × *g* at 4 °C for 15 min. The cells were washed twice in Tris medium; washing fluids were eliminated by centrifugation. The washed cells were resuspended in Tris medium with glucose and left to grow for 2 h. The samples (1 ml) were taken at the indicated times, and bacterial cells were treated as described above. Whole cell extracts (25 μg protein) were analyzed by native PAGE in 10% acrylamide and Tris-glycine buffer. Protein concentration was determined by the Bradford method (41). The dried gels were autoradiographed at −80 °C, for 48 h, using KODAK BioMax XAR films. For each bacterial strain, six independent time course experiments were performed. The autoradiograms shown are representative of one experiment. For each time point, the amount of $^{59}$Fe bound to relevant proteins was determined by scintillation counting of the excised bands from the gels. The results are given as the relative percentages of total counts measured on the gels, for each lane. The data reported are the averages of six independent experiments, and the standard deviations are indicated.

*Immunodetection of the Bfr Protein*—Proteins (25 μg) were loaded and run onto 15% polyacrylamide 0.1% SDS denaturating gels. The proteins were transferred onto nitrocellulose membranes (Protran BA 83; Whatman) at 350 mA for 75 min in 30 mM Tris, 192 mM glycine, 0.025% SDS, 20% v/v methanol, pH 8.3, using the Bio-Rad mini-Trans-Blot electrophoretic transfer cell. Bfr antiserum was used at a dilution of 1/4000. Antibody binding was detected with goat anti-rabbit immunoglobulin conjugated to alkaline phosphatase.

*Analysis of FMP Iron and Mass Spectrometry*—Bands corresponding to the $^{59}$Fe-labeled proteins doublet detected by autoradiography of native gels were cut out (Fig. 5*A*, *panel 1*) and analyzed by SDS-PAGE in 10% acrylamide and Tris-glycine buffer (Fig. 5*A*, *panel 3*), as described by Schägger and Von Jagow (42). The gels were stained with Coomassie Blue. For control experiments, the protein bands excised from the gel were analyzed a second time on native PAGE (Fig. 5*A*, *panel 2*) to check for the presence of a $^{59}$Fe spot corresponding to the protein doublet detected on the first gel. Individual spots visualized after SDS-PAGE were excised, reduced with dithiothreitol, alkylated with iodoacetamide, and digested with trypsin overnight at 37 °C. Tryptinized peptides were extracted from the gel pieces with 50% acetonitrile, 0.1% trifluoroacetic acid, concentrated, desalted, using a ZipTip (Millipore, Molsheim, France), and spotted onto a steel target with α-cyano-4-hydroxycinnamic acid as a matrix. The peptide mass fingerprint was acquired after external calibration with ions from des-Arg$^1$-Bradykinin, Angitensin I, Glu$^1$-Fibrinopeptide B, and neurotensin, on a 4800 TOF-TOF spectrometer (Applied Biosystems) equipped with a YAG-200 Hz laser (355 nm). Operating parameters for the Reflectron included 1500 laser shots/spectrum. Monoisotopic masses were used with a maximum deviation of ± 100 ppm for mass assignment. For protein identification, the peptide mass fingerprint was searched against the ASAP data base, using Mascot (Matrix Science, London, UK). Protein hits were accepted if the Mascot score was greater than the significance threshold. This procedure was carried out in six independent samples isolated from cytosolic extracts of parental cells supplied with $^{59}$Fe-chrysobactin at concentrations of 0.25 μM, for 40 min.

*Transport Assays*—Bacterial cultures were grown in the same conditions used for *in vivo* labeling experiments. Transport assays were carried out as described by Rauscher *et al.* (43), with the addition of $^{59}$Fe-labeled chrysobactin to the transport medium at a concentration of 0.25 μM.

*Enzyme Assays*—Aconitase activity was assayed in bacterial pellets from 100-ml cultures grown in the conditions indicated and stored at −80 °C for 24 h, as described by Gardner (44). The protein concentration was determined by the Bradford method.

## RESULTS

*Intracellular Distribution of Iron in Cells Supplied with $^{59}$Fe-Chrysobactin*—Previous studies have shown that the ferric chrysobactin complex is dissociated inside the cell through a rapid reductive process, making iron available for metabolic needs (43). Thus, we used $^{59}$Fe-chrysobactin to try to identify intracellular protein targets of iron in *E. chrysanthemi* cells. We used a double mutant strain deficient in biosynthesis of both chrysobactin and achromobactin (PPV20) to avoid iron exchange between both ligands. In the low iron minimal Tris medium, the doubling time of this mutant was 160 min. The addition of ferric chrysobactin to the medium stimulated the growth rate, the doubling time being 100 min. Cytosolic protein extracts were analyzed by PAGE on nondenaturing gels, and protein-bound iron was visualized by autoradiography as described under "Experimental Procedures." We first tested a concentration range of 0.06–1 μM $^{59}$Fe-chrysobactin added over a period of 40 min (Fig. 1*A*). We detected a continuum of bands increasing in intensity with higher $^{59}$Fe concentrations, which could correspond to the banding region revealed by Coomassie Blue staining. In addition, two strong $^{59}$Fe signals (designated as *1* and *2* on Fig. 1*A*), a slowly migrating protein species and a quickly migrating protein doublet, were apparent. A third signal (designated as *3* on Fig. 1*A*) became visible with concentrations of $^{59}$Fe higher than 0.125 μM. We then performed a time course experiment. Protein-bound iron was probed at 10-min intervals over a 40-min period after adding 0.25 μM $^{59}$Fe-chrysobactin (Fig. 1*B*). We observed the same $^{59}$Fe signals increasing in intensity with time. Thus, iron binds a wide vari-

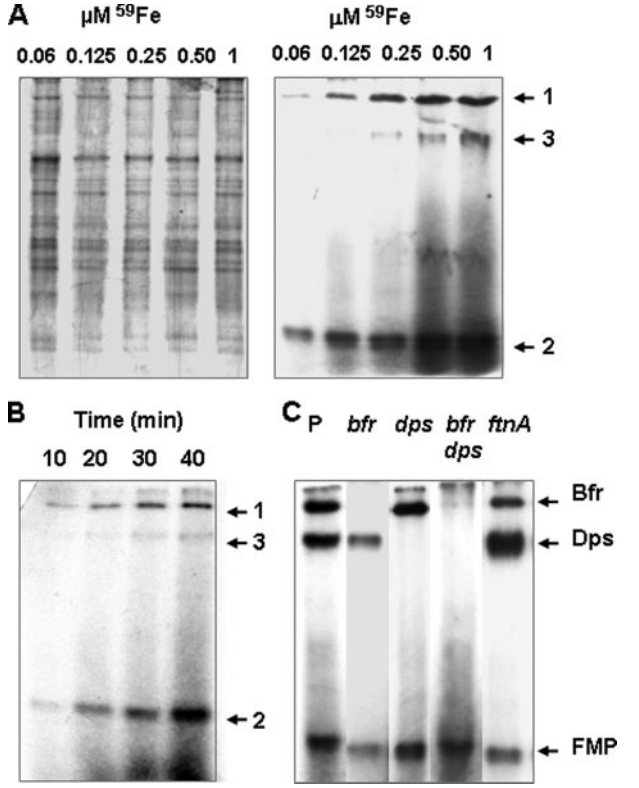


FIGURE 1. **Native PAGE analysis of protein extracts from *E. chrysanthemi* cells supplied with $^{59}$Fe-chrysobactin.** Protein-bound iron was detected by autoradiography. Further details are described under "Experimental Procedures." *A*, $^{59}$Fe-chrysobactin was supplied to parental cells at the indicated concentrations for 40 min. The autoradiogram shown in the *right panel* corresponds to proteins visualized by Coomassie Blue staining in the *left panel*. *B*, 0.25 $\mu$M $^{59}$Fe-chrysobactin was supplied to parental cells for the indicated times. *C*, parental and relevant mutant cells (as indicated by *P* and corresponding genotypes) were supplied with 1 $\mu$M $^{59}$Fe-chrysobactin for 40 min. Insoluble material is visible at the *tops* of some lanes. $^{59}$Fe-labeled signals are designated by *arrows 1*, *2*, and *3*, respectively.

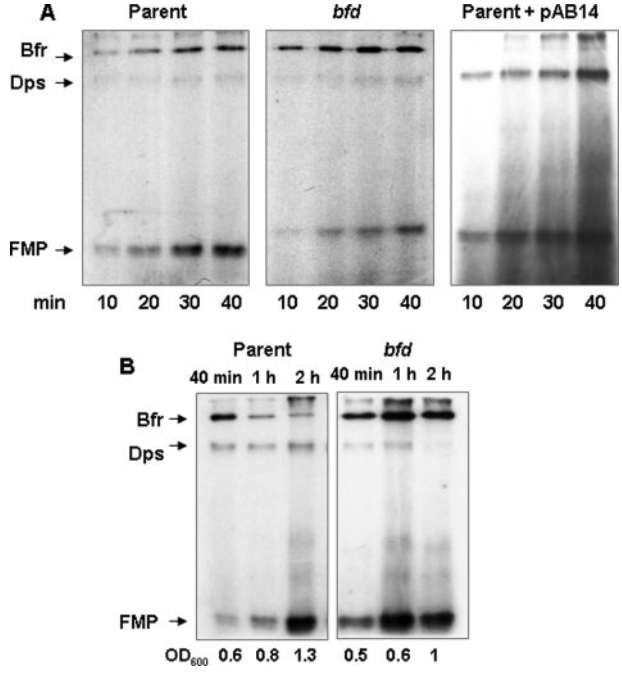


FIGURE 2. **Distribution of iron in bacterioferredoxin-proficient and -deficient cells supplied with $^{59}$Fe-chrysobactin.** Native PAGE analysis of protein extracts was performed as described in Fig. 1. *A*, $^{59}$Fe-chrysobactin was supplied at the concentration of 0.25 $\mu$M for the indicated times. *B*, $^{59}$Fe-chrysobactin was supplied at the concentration of 0.5 $\mu$M for 40 min as indicated. The cells were then washed and grown for the indicated times (details are under "Experimental Procedures"); optical density at 600 nm ($OD_{600}$) of bacterial cultures is indicated. The strains are designated as in Fig. 1. Plasmid pAB14 contains the *bfd* gene under the control of its own promoter.

ety of proteins. Those referred to as signals 1 and 3 could be ferritin-like compounds.

To test this possibility, we performed similar experiments with *bfr*, *dps*, and *ftnA* mutant strains carrying defects in the production of Bfr, Dps, or FtnA protein (PPV51, PPV52, and PPV53), respectively. Iron-deprived bacterial cells were supplied with 0.25 $\mu$M $^{59}$Fe-chrysobactin for 40 min, and protein-bound iron was analyzed (supplemental Fig. S1). Signal 1, identified in the parental strain as a slowly migrating protein, was absent from the *bfr* mutant but present in *dps* and *ftnA* mutants, suggesting that this protein could be Bfr. Signal 3 (Fig. 1, *A* and *B*), another slowly migrating protein identified in the parental strain, was present in the *ftnA* mutant but absent from the *dps* mutant. This signal was therefore likely to correspond to Dps. A *fur* mutant, which displays a low level of transcriptional activity of the *bfd-bfr* operon, showed a particularly strong Dps signal (supplemental Fig. S1). To confirm these data, we increased the concentration of $^{59}$Fe-chrysobactin in the medium to 1 $\mu$M and compared the signal patterns obtained from mutant strains to those from the parental strain (Fig. 1*C*). In the parental strain, the signals corresponding to Bfr and Dps were strong, whereas they were absent from the respective mutants. Both signals were absent from the *bfr dps* double mutant (PPV54) (Fig. 1*C*). The doublet corresponding to the quickly migrating protein species was present in all of the mutant strains. Its signal intensity increased over time, as observed for the parental strain (supplemental Fig. S1). Thus, some of the iron released from chrysobactin is sequestered by Bfr, Dps, and a set of proteins unrelated to ferritins, designated FMP. The amounts of $^{59}$Fe bound to these various protein species were quantified (supplemental Table S2). In parental cells supplied with 0.25 $\mu$M $^{59}$Fe-chrysobactin for 40 min, iron bound to Bfr represented ~5%, Dps iron represented ~1%, and FMP iron 16% of total $^{59}$Fe detected on the gels. In the *bfr* mutant, levels of FMP iron were similar to those of the parent strain, whereas they reached 20% in the *dps* mutant. In the *fur* mutant, iron bound to Dps and FMP represented 16 and 20% of total $^{59}$Fe signal, respectively. We did not detect iron bound to FtnA, probably because the *ftnA* gene is not expressed in iron-deprived cells (32).

*Release of Iron from Bacterioferritin Requires Bacterioferredoxin*—The roles of bacterioferritin and bacterioferredoxin in iron metabolism are not well understood. As in *E. coli*, *E. chrysanthemi* bacterioferritin is not involved in long term iron storage (21, 32). To gain insight into the roles of these proteins, we constructed a nonpolar *bfd*-negative mutant (PPV55) and examined the distribution of iron in this mutant, and in the parental strain, over time. Cultures of iron-depleted cells were supplied with 0.25 $\mu$M $^{59}$Fe-chrysobactin for 40 min (Fig. 2*A*). In the *bfd* mutant, the signal intensity for Bfr-bound iron was 2.8 times greater than in the parental strain. However, the intensity of signals corresponding to Dps and FMP, was similar in both strains (supplemental Table S2). We carried out the same

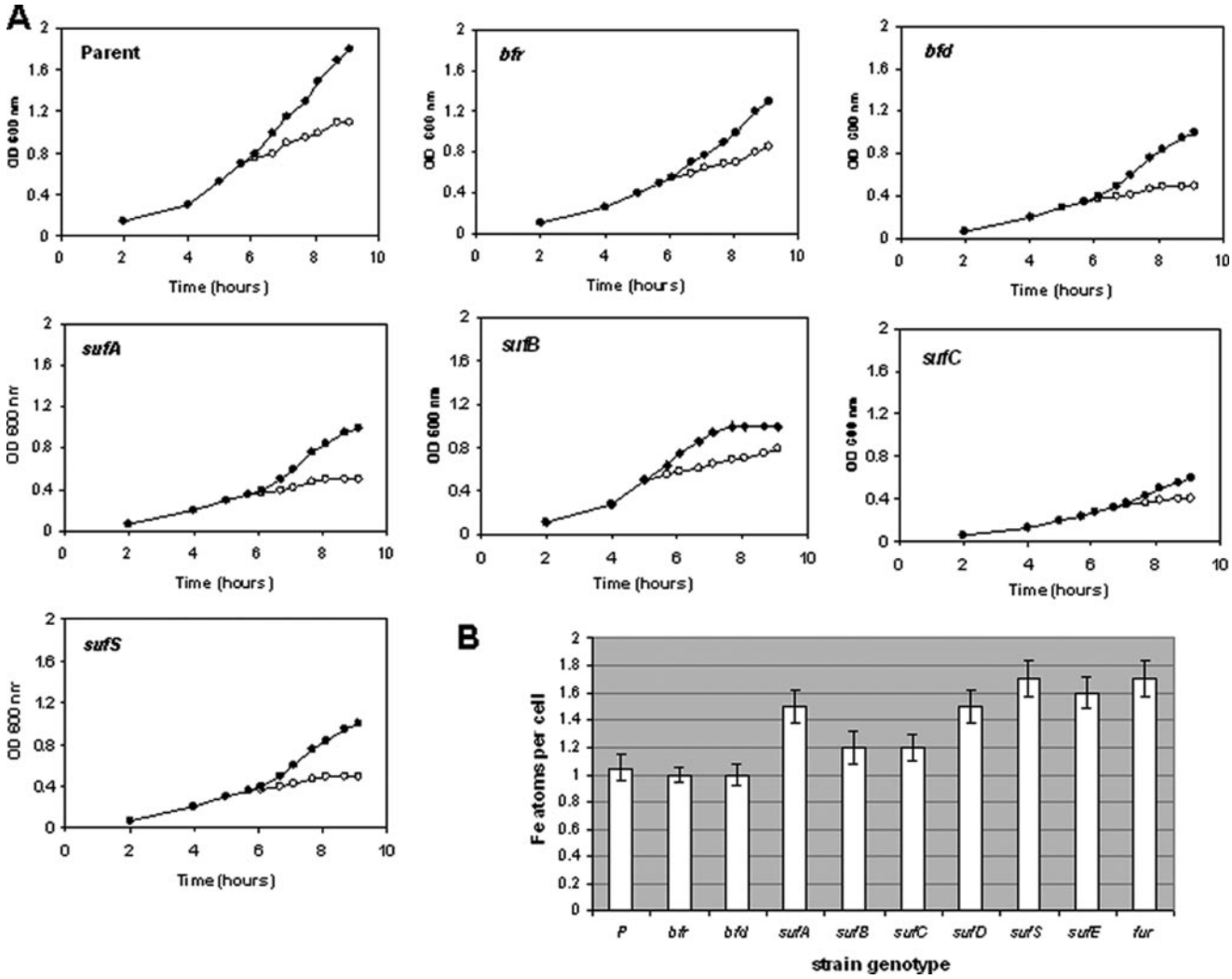


FIGURE 3. **Growth and transport characteristics of parental and relevant mutant strains treated with $^{59}$Fe-chrysobactin.** *A*, growth of bacterial cultures with (*solid circles*) or without (*open circles*) the addition of 1 $\mu$M $^{59}$Fe-chrysobactin. $^{59}$Fe-chrysobactin was added when $A_{600} = 0.4$. Genotypes are shown on each graph. Growth curves of the *sufD* and *sufE* mutants (not shown) were similar to those obtained for the *sufB* and *sufS* mutants, respectively. The experiments were performed five times, and the data reported are the means of three independent experiments with standard deviation corresponding to less than 5%. *B*, amounts of iron ($\times 10^6$ atoms) incorporated into parental and relevant mutant cells after treatment with 0.25 $\mu$M $^{59}$Fe-chrysobactin for 40 min. Transport assays were performed as described under "Experimental Procedures." The data are the means of measurements obtained in three separate experiments, with *error bars* representing S.D.

experiment with a bacterial construct containing extra copies of the *bfd* gene expressed on a multicopy plasmid (pAB14) (Fig. 2*A*). The signal intensity for Bfr iron was strongly reduced, whereas that observed for Dps was increased. We then analyzed the fate of iron at different stages of cell growth. Iron-depleted cultures from the parental strain and the *bfd* mutant were treated with 0.5 $\mu$M $^{59}$Fe-chrysobactin for 40 min. The cells were washed and grown in fresh iron-free medium for an additional 2 h (see "Experimental Procedures"). Protein-bound iron was analyzed at 40 min, 1 h, and 2 h after washing (Fig. 2*B*). In parental cells, the signal intensity for Bfr iron progressively decreased, indicative of the metal being released during cell growth. We did not observe this effect in *bfd* cells. This suggests that bacterioferredoxin is required for iron release from bacterioferritin. The absence of Bfr-bound iron from cells overexpressing the *bfd* gene is likely to be due to overproduction of the Bfd protein causing an exacerbation of the release process. These data highlight the importance of a clustered organization of the *bfd* and *bfr* genes in an operon, allowing the coordinated production of Bfd and Bfr proteins.

*Delivery of Iron to Bacterioferritin Is Impaired in Nonpolar sufA, sufB, sufD, sufS, and sufE Mutants*—The *sufABCDSE* operon is involved in iron-sulfur cluster biogenesis and is iron-regulated (13). Thus, we determined whether the absence of Suf proteins led to changes in intracellular iron distribution. We first compared the growth of nonpolar *sufA to sufE* negative mutants (PPV56–PPV61) and *bfr* and *bfd* mutants (PPV51 and PPV55) in Tris medium, with or without ferric chrysobactin, with that of parental strain (Fig. 3*A*). In Tris medium, all of the strains grew slowly, although to various extents depending on the genotype. Cell growth was most severely affected in the *sufA*, *sufC*, *sufS*, and *bfd* mutants ($p$ value $\leq 0.03$). The addition of ferric chrysobactin greatly stimulated growth of the parental strain and to a lesser extent that of the mutants. Growth of the *sufC* mutant was only mildly stimulated. To confirm that these growth defects were not caused by impaired ferric chrysobactin

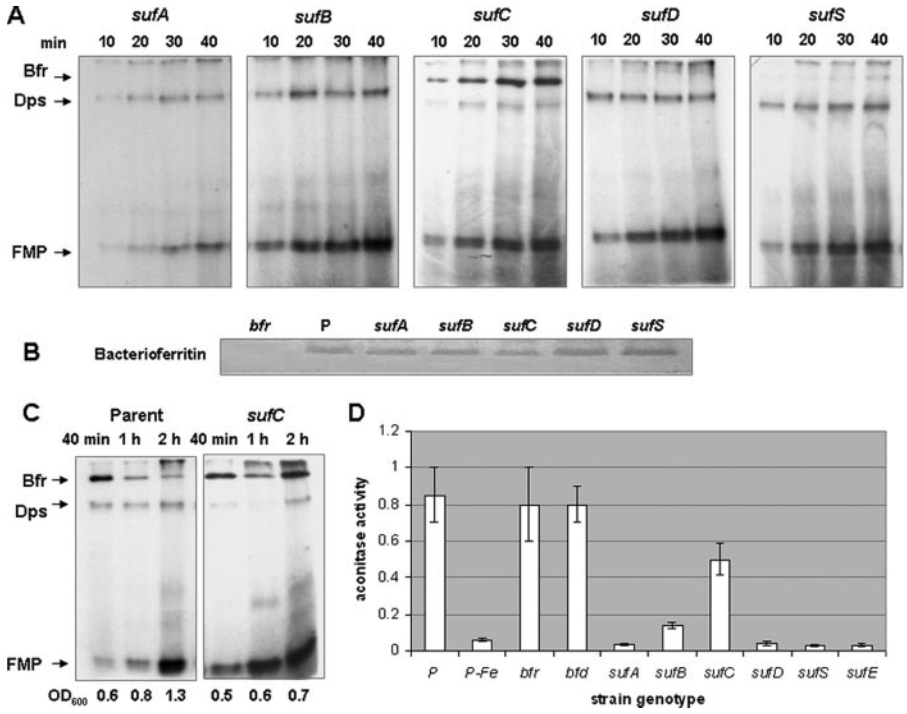


FIGURE 4. **Iron metabolism in *suf* negative mutants supplied with $^{59}$Fe-chrysobactin.** *A*, native PAGE analysis of protein extracts was performed as described in Fig. 1. $^{59}$Fe-chrysobactin was supplied at the concentration of 0.25 $\mu$M for the indicated times. *B*, immunoblotting of bacterioferritin in protein extracts from $^{59}$Fe-chrysobactin-treated cultures of relevant strains. *C*, native PAGE analysis of protein extracts from *sufC* cells was performed as described for Fig. 2*B*. *D*, aconitase activity produced in parental and relevant mutant cells. Enzyme activity was assayed in cells from iron-deprived cultures treated with 0.5 $\mu$M $^{59}$Fe-chrysobactin for 4 h. For the parental strain, enzyme activity was assayed with no iron supplementation (*P-Fe*). One unit of aconitase activity corresponds to the conversion of 1 $\mu$mol of citrate to isocitrate/min; specific activity is given in units/mg of protein/min. The data are the means of measurements obtained in three separate experiments with *error bars* representing S.D. The relevant genotypes are indicated.

transport, we quantified the iron incorporated into bacterial cells after treatment with 0.25 $\mu$M $^{59}$Fe-chrysobactin for 40 min (Fig. 3*B*). Parental and *bfr*- and *bfd*-deficient cells contained similar amounts of total $^{59}$Fe. In the *sufA*, *sufD*, *sufS*, *sufE*, and *fur* mutants, $^{59}$Fe levels were 40% higher than those in the parental strain ($p$ value $\leq$ 0.04). *sufS* and *sufE* mutants had similar levels to those observed in the *fur* mutant, in which iron transport is derepressed.

We then analyzed the distribution of iron in the *suf* negative mutants (PPV56–PPV61) over time. Iron-depleted cultures from the mutants were treated with 0.25 $\mu$M $^{59}$Fe-chrysobactin for 40 min, and protein iron was analyzed (Fig. 4*A*). We did not detect a signal corresponding to Bfr-bound iron in *sufA* and *sufB* mutants, and the signal in the *sufD*, *sufS*, and *sufE* mutants was very weak. The amount of Dps-bound iron was higher in these mutants than in the parental strain (Fig. 4*A* and supplemental Table S2). In the *sufC* mutant, iron sequestered by Bfr seemed to accumulate over time; the amount of Bfr iron measured at 30 min was twice as high as that observed for the parental strain. The amount of Dps iron in this mutant was similar to that of the parental strain. FMP iron was detected in all *suf* mutants. The amount of FMP iron was higher in the *sufC*, *sufS*, and *sufE* mutants than in the parental strain. We checked by immunoblotting that the lack of Bfr iron in the *suf* mutants was not due to the absence of Bfr protein (Fig. 4*B*). Given that the *sufC* mutant was able to accumulate more iron in bacterioferritin than the parent strain, we examined the turnover of this metal during cell growth, as described for the *bfd* mutant above. We did not observe the release of iron from bacterioferritin during cell growth (Fig. 4*C*). Thus, the *sufC* and *bfd* mutations result in a similar phenotype involving a defect in iron release from bacterioferritin.

*Aconitase Activity Is Impaired in Nonpolar sufA, sufB, sufD, sufS, and sufE Mutants*—To determine whether iron recycled from bacterioferritin is essential to the formation of iron-sulfur clusters through the Suf pathway, we measured aconitase activity in parental and mutant strains. *E. chrysanthemi* contains an ortholog of the *E. coli* aconitase B-encoding gene *acnB*. Aconitase B is a member of the iron-sulfur-containing protein family (45). We determined the activity of this enzyme in cell extracts of iron-depleted cultures treated with or without ferric chrysobactin in the parental strain (Fig. 4*D*). Ferric chrysobactin-treated cultures displayed significant levels of aconitase activity, whereas aconitase activity was 10 times lower in cells exposed to the conditions of iron depletion. The aconitase activity in ferric chrysobactin-treated *sufA*, *sufD*, *sufS*, and *sufE* mutant cultures was also very low. That of the *sufC* mutant, however, was only reduced by a factor of 2 ($p$ value $\leq$ 0.04). This indicates that the SufC protein is not essential for the assembly of iron-sulfur clusters or their transfer to apo-aconitase. The aconitase activity measured in ferric chrysobactin-treated cultures of the *bfr* and *bfd* mutants was similar to that of the parent, indicating that the Bfr-Bfd system is not essential for providing the Suf machinery with iron.

*Characterization of FMP Iron Pool*—The $^{59}$Fe-labeled doublet detected on native gel was further resolved to reveal its individual polypeptides by denaturing SDS-PAGE as described under "Experimental Procedures" and in Fig. 5*A*. We identified several spots, ranging from 3 to 10, depending on the experiment considered. The corresponding polypeptides were analyzed by mass spectrometry. These polypeptides were related to basic biological processes, such as protein translation and folding, energy/carbon metabolism, amino acid biosynthesis, and potential metal ion binding (supplemental Table S3). FMP iron may thus play a role in protein translation. Given that magnesium ions contribute to maintenance of the 50 S ribosomal architecture and is necessary for EF-Tu protein chain elongation activity (46, 47), we checked that ferrous ions were not replacing magnesium ions. Increasing the magnesium concentration in the culture medium up to 20 mM, *i.e.* 0.5 mM in Tris medium, did not affect formation of this pool (Fig. 5*B*). We analyzed the effect of antibiotics - fusidic acid, which blocks

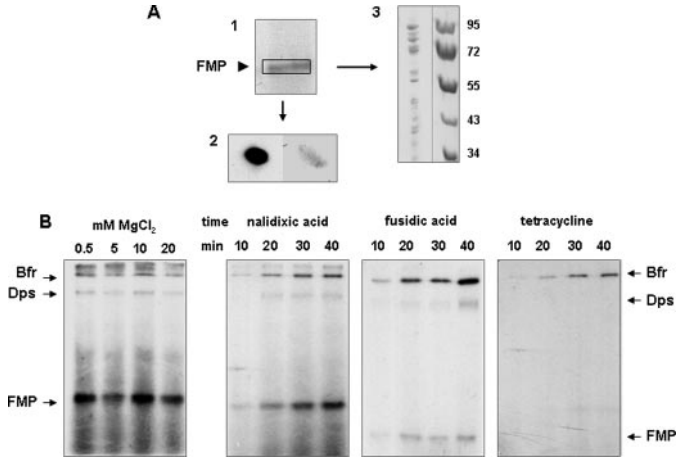


FIGURE 5. **FMP iron analysis.** *A*, FMP iron was analyzed as described under "Experimental Procedures." *Panel 1*, excision of the gel band corresponding to signal 2 in Fig. 1*B*; *panel 2*, second migration on native gel: autoradiogram (*left side*) and Coomassie Blue staining (*right side*); *panel 3*, individual spots revealed by Coomassie Blue staining after SDS-PAGE (*left lane*): from *top* to *bottom*, EF-G factor, aconitase, 30 S ribosomal protein S1, HSP-90, trigger factor, arginosuccinate synthetase, serine hydroxymethyltransferase, aspartate-semialdehyde dehydrogenase. The apparent molecular sizes of standard proteins (*right lane*) in kDa are indicated. *B*, distribution of iron in parental cells exposed to agents inhibiting protein translation. Native PAGE analysis of protein extracts was performed as described in Fig. 1. The cells were grown in Tris medium containing the concentrations of $MgCl_2$ indicated, and $^{59}$Fe-chrysobactin was supplied at the concentration of 0.125 $\mu$M. Nalidixic acid, fusidic acid, and tetracycline were added to bacterial cultures at a concentration of 10 $\mu$g, 1.2 mg, and 2.5 $\mu$g/ml respectively, 5 min before the addition of 0.5 $\mu$M $^{59}$Fe-chrysobactin.

EF-G-mediated translocation of peptidyl-tRNA on the ribosome, and tetracycline, which disrupts codon/anticodon interactions - on this iron pool (48, 49) (Fig. 5*B*). These drugs were added to cultures 5 min before adding $^{59}$Fe-chrysobactin. Formation of the pool of FMP iron was severely disrupted. The continuum of bands was also strongly reduced, whereas the pool of iron bound to bacterioferritin remained unchanged. Nalidixic acid, an inhibitor of DNA gyrase (50), had no effect. Thus, *de novo* protein biosynthesis is required for detection of $^{59}$Fe signals corresponding to FMP and to the continuum of protein bands.

## DISCUSSION

In this study, we investigated the intracellular fate of iron transported by a siderophore-mediated pathway. We provide a model demonstrating the management of iron in bacterial cells during a period of transition, in this case from conditions of iron depletion to iron repletion. We identified a functional link between the Suf machinery and the bacterioferritin-bacterioferredoxin system, which results in a balanced distribution of iron to its protein targets and optimization of the metabolic role of this metal.

We used PAGE under nondenaturing conditions to detect $^{59}$Fe-labeled proteins in soluble extracts from *E. chrysanthemi* cells supplied with $^{59}$Fe via chrysobactin. We observed a diverse range $^{59}$Fe signals differing in intensity, visualized as a continuum of faint bands and intense bands corresponding to FMP iron and iron bound to bacterioferritin and mini-ferritin. At 40 min after the addition of the iron source, ~78% of total $^{59}$Fe counts measured on the gels could be attributed to this continuum, ~16% could be attributed to FMP, 5% to bacterioferritin, and 1% to mini-ferritin. The amounts of iron associated to the continuum and to FMP were strongly reduced by inhibiting protein translation with antibiotics. These data suggest that incoming iron is delivered to a wide range of protein species visualized as a continuum, which probably includes many metalloenzymes and other metalloproteins. This process requires *de novo* protein biosynthesis; thus, the delivery of iron to these targets seems to be mediated by newly synthesized intracellular metal carrier(s). It is also possible that the whole continuum of bands corresponds to a pool of newly translated proteins having acquired their iron cofactor. This possibility fits with the presence of the FMP iron pool, also resulting from *de novo* protein biosynthesis. However, we were surprised not to find that iron-binding proteins could account for the high metal content observed in this pool. The isolated proteins were involved in basic cellular processes such as protein translation and folding, carbon metabolism, amino acid biosynthesis, and possibly metal ion binding. They must be the most abundant species in cells recovering active metabolism. Iron-starved cells are metabolically weak. The addition of $^{59}$Fe-chrysobactin rapidly stimulated growth in the parental strain, indicative of metabolic rescue (Fig. 3). Consistent with this, signal corresponding to FMP iron was weak when bacterial cells were grown in rich medium supplemented with $^{59}$Fe (data not shown). This suggests that the strong $^{59}$Fe signal observed for the FMP pool results from an accumulation of iron because of a set of iron-binding proteins migrating together on native gels. The amount of each protein species would be too low to be detectable. An alternative but not exclusive possibility would be the presence of low levels of an unknown protein able to accommodate high levels of iron. Further investigations are required to address these issues.

Bacterioferritin and to a lesser extent mini-ferritin also appear as primary targets of intracellular iron delivery, indicating that these iron storage proteins are important in the metabolism of iron-starved cells. In the absence of bacterioferritin, as in the *bfr* mutant, mini-ferritin can store more iron. This effect is particularly marked in a *fur* mutant that has increased levels of Dps-bound iron, probably because of the constitutive expression of its iron transport proteins (Fig. 3*B*), reduced transcription of the *bfr* gene (32), and increased transcription of the *dps* gene.[4] The role played by the bacterioferritin is interesting. Indeed, we found that iron bound to this protein was absent from *sufA*, *sufB*, and *sufD* mutants and strongly reduced in mutants harboring a *sufS* or *sufE* mutation. This defect was not due to the absence of Bfr protein, as shown by immunoblotting. By contrast, the *sufC* mutant displays increased levels of Bfr iron. This suggests that the Suf components, with the exception of SufC, are involved in the transfer of iron to bacterioferritin. Although the importance of Suf machinery in iron-sulfur cluster assembly under conditions of iron limitation is established, the mechanisms underlying Suf protein function *in vivo* are poorly understood. In the model proposed by Layer *et al.* (51), SufS is a cysteine desulfurase that releases sulfur from cysteine

[4] D. Expert, A. Boughammoura, and T. Franza, unpublished observations.

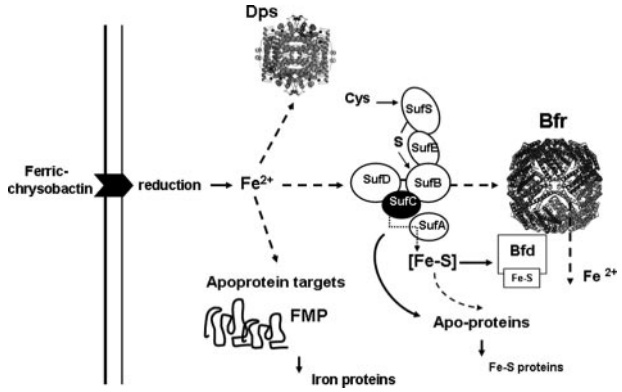


FIGURE 6. **Model for intracellular distribution of iron between protein targets, in iron-deprived cells supplied with ferric chrysobactin.** See text for details. This model is built on the basis of published data on ferric chrysobactin processing (43), Suf protein-protein interactions during iron-sulfur cluster assembly (51), and bacterioferredoxin redox catalyst function (34, 52). The *dashed line arrows* indicate possible routes of iron trafficking between target proteins. The *solid line arrow* indicates the role of SufC in the formation of iron-sulfur proteins. The possible involvement of additional iron trafficking proteins is not depicted.

and SufE is a sulfur transfer protein donating sulfur to SufB and SufA (Fig. 6). SufB and SufA can act as scaffolding proteins and mediate transfer of clusters to target apoproteins. SufC is an ATPase subunit of the ABC transporter family able to form a complex with both SufB and SufD. SufB can also interact with SufE if SufC is present. It remains to be determined how iron is handled by this machinery.

Thus, we can propose a model involving the release of iron from the siderophore, its transfer to the Suf pathway, possibly via SufA, SufB, and/or SufD, followed by its incorporation by bacterioferritin. Bfr iron seems to be recycled through the action of bacterioferredoxin, because iron release from Bfr was compromised in a *bfd* mutant. This is consistent with previous data showing that the *E. coli* Bfd protein can physically interact with Bfr and acts as a redox catalyst (34, 52). However, iron recycled through the Bfr-Bfd pathway does not seem to be essential for the function of Suf machinery, given that the *bfd* mutation had no effect on the production of aconitase. The role of the SufC component could be to facilitate the formation of iron sulfur clusters and/or their transfer to apotargets, a function that is reminiscent of that of the ATPase ApbC from *S. enterica* (53). Indeed, aconitase activity in the *sufC* mutant is only reduced by a factor of two, demonstrating that the Suf machinery, although less efficient, is still functional. This mutant, similarly to the *bfd* mutant, has defective iron recycling from bacterioferritin. Thus, the production of bacterioferredoxin may be impaired in the *sufC* mutant, a defect that could be due to the reduced capacity of this strain to produce or to transfer iron-sulfur clusters. The validity of this model implies that Suf, Bfr, and Bfd proteins cooperate in various configurations *in vivo*, although other iron trafficking proteins may be involved. In *E. coli*, the protein NfuA could act as a scaffold/chaperone for the insertion of iron-sulfur clusters into target proteins (54). Thus, the role of the *E. chrysanthemi* NfuA protein has to be elucidated. Other findings suggest that the YggX small protein identified in *Salmonella enterica* for its protective role against oxidative stress facilitates iron trafficking to appropriate cellular locations (55–57). The *E. chrysanthemi* genome encodes an YggX homolog. Further study is needed to determine the potential role of this protein. Nevertheless, the YggX protein binds ferrous ions only weakly, and thus a role in iron trafficking is unlikely (58). Another possible candidate is the homolog of Ytfe, a di-iron protein conserved in enterobacteria and present in *E. coli* under conditions of nitrosative stress and iron starvation (59, 60).

All of the mutations studied impairing the Bfr-Bfd pathway or the Suf components reduced cell growth even under conditions of iron supplementation with chrysobactin. These mutations have no effect on ferric chrysobactin transport *per se*; therefore the observed phenotypes result from impaired intracellular iron management. Indeed, the *sufA*, *sufB*, *sufD*, *sufS*, and *sufE* mutants have a deficit in iron-sulfur clusters and cannot store iron through sequestration by bacterioferritin, even after 3 h of iron supply (data not shown). Growth of the *sufC* mutant was severely affected, although it still produces significant levels of aconitase. In fact, this mutant is particularly sensitive to oxidative conditions, including agents like streptonigrin (13). However, unlike the *sufA*, *sufD*, *sufS*, and *sufE* mutants, it did not accumulate more iron than normal (Fig. 3*B*). This suggests that the reduced growth of this mutant could be due to the activity of the other Suf proteins causing accumulation of incompletely processed iron-sulfur clusters prone to oxidative damage (3). Cell growth was also significantly impaired in the *bfd* mutant to a greater extent than that observed for the *bfr* mutant. Thus, the Bfr-Bfd pathway seems to be needed for a rapid turnover and optimized intracellular utilization of iron.

In conclusion, the selective incorporation of iron into iron-sulfur cluster proteins and other proteins requiring this metal as a cofactor involves the action of Suf components, Bfr and Bfd proteins. This can be beneficial to many pathogens for growth in a host environment that is continually changing in terms of iron availability and redox conditions.

*Acknowledgments—We thank J.-M. Camadro and J.-J. Montagne for access to the Plateforme Protéomique (Institut Jacques Monod, CNRS-Universités Paris 6 and 7) and helpful discussions. We thank S. Andrews for the gift of E. coli bacterioferritin antiserum. We are grateful to B. Matzanke for its interest in this work. We are grateful to J. Gray for English reading of the manuscript.*

## REFERENCES

1. Neilands, J. B. (1991) *Biol. Met.* **4,** 1–6
2. Pierre, J.-L., and Fontecave, M. (1999) *BioMetals* **12,** 195–199
3. Imlay, J. A. (2003) *Annu. Rev. Microbiol.* **57,** 395–418
4. Faraldo-Gomez, J. D., and Sansom, M. S. P. (2003) *Nat. Rev. Mol. Cell. Biol.* **4,** 105–116
5. Krewulak, K. D., and Vogel, H. J. (2008) *Biochim. Biophys. Acta* **1778,** 1781–1804
6. Lee, J. W., and Helmann, J. D. (2007) *BioMetals* **20,** 485–499
7. Miethke, M., and Marahiel, M. A. (2007) *Microbiol. Mol. Biol. Rev.* **71,** 413–451
8. Barras, F., Loiseau, L., and Py, B. (2005) *Adv. Microb. Physiol.* **50,** 41–101
9. Ayala-Castro, C., Saini, A, and Outten, F. W. (2008) *Microbiol. Mol. Biol. Rev.* **72,** 110–125
10. Frazzon, A. P., Ramirez, M. V., Warek, U., Balk, J., Frazzon, J., Dean, D. R., and Winkel, B. S. J. (2007) *Plant Mol. Biol.* **64,** 225–240

11. Johnson, D. C., Dean, D. R., Smith, A. D., and Johnson, M. K. (2005) *Annu. Rev. Biochem.* **74,** 247–281
12. Fontecave, M., Ollagnier de Choudens, S., and Barras, F. (2005) *J. Biol. Inorg. Chem.* **10,** 713–721
13. Nachin, L., El Hassouni, M., Loiseau, L., Expert, D., and Barras, F. (2001) *Mol. Microbiol.* **39,** 960–972
14. Outten, F. W., Djaman, O., and Storz, G. (2004) *Mol. Microbiol.* **52,** 861–872
15. Yeao, W.-S., Lee, J.-H., Lee, K.-C., and Roe, J.-H. (2006) *Mol. Microbiol.* **61,** 206–218
16. Layer, G., Ollagnier de Choudens, S., Sanakis, Y., and Fontecave, M. (2006) *J. Biol. Chem.* **281,** 16256–16263
17. Ding, H., Yang, J., Coleman, L. C, and Yeung, S. (2007) *J. Biol. Chem.* **282,** 7997–8004
18. Gerber, J., Mühlenhoff, U., and Lill, R. (2003) *EMBO Rep.* **4,** 906–911
19. Foury, F., Pastore, A., and Trincal, M. (2007) *EMBO Rep.* **8,** 194–199
20. Matzanke, B. F. (1997) in *Transition Metals in Microbial Metabolism* (Winkelmann, G., and Carrano, C. J., eds) pp. 117–158, Harwood Academic Publishers GmbH, Amsterdam, The Netherlands
21. Andrews, S. C., Robinson, A. K., and Rodriguez-Quinones, F. (2003) *FEMS Microbiol. Rev.* **27,** 215–237
22. Chiancone, E., Ceci, P., Ilari, A., Ribacchi, F., and Stefanini, S. (2004) *BioMetals* **17,** 197–202
23. Smith, J. L. (2004) *Crit. Rev. Microbiol.* **30,** 173–185
24. Carrondo, M. A. (2003) *EMBO J.* **22,** 1959–1968
25. Le Brun, N. E., Andrews, S. C., Guest, J. R., Harrison, P. M., Moore, G. R., and Thomson, A. J. (1995) *Biochem. J.* **312,** 385–392
26. Ilari, A., Stefanini, S., Chiancone, E., and Tsernoglou, D. (2000) *Nat. Struct. Biol.* **7,** 38–43
27. Stillman, T. J., Connolly, P. P., Latimer, C. L., Morland, A. F., Quail, M. A., Andrews, S. C., Hudson, A. J., Treffry, A., Guest, J. R., and Harrison, P. M. (2003) *J. Biol. Chem.* **278,** 26275–26286
28. Liu, X., and Theil, E. C. (2004) *Proc. Natl. Acad. Sci. U. S. A* **101,** 8557–8562
29. Expert, D. (1999) *Annu. Rev. Phytopathol.* **37,** 307–334
30. Franza, T., Mahé, B., and Expert, D. (2005) *Mol. Microbiol.* **55,** 261–275
31. Nachin, L., Loiseau, L., Expert, D., and Barras, F. (2003) *EMBO J.* **22,** 427–437
32. Boughammoura, A., Matzanke, B., Böttger, L., Reverchon, S., Lesuisse, E., Expert, D., and Franza, T. (2008) *J. Bacteriol.* **190,** 1518–1530
33. Andrews, S. C., Harisson, P. C., and Guest, J. R. (1989) *J. Bacteriol.* **171,** 3940–3947
34. Garg, P. R., Vargo, C. J., Cui, X., and Kurtz, D. M. (1996) *Biochemistry* **35,** 6297–6301
35. Franza, T., Enard, C., Van Gijsegem, F., and Expert, D. (1991) *Mol. Microbiol.* **5,** 1319–1329
36. Sambrook, J., Fritsch, E. F., and Maniatis, T. (1989) *Molecular Cloning: A Laboratory Manual*, 2nd Ed., Cold Spring Harbor Laboratory, Cold Spring Harbor, NY
37. Franza, T., Sauvage, C., and Expert, D. (1999) *Mol. Plant-Microbe Interact.* **12,** 119–129
38. Résibois, A., Colet, M., Faelen, M., Schoonejans, E., and Toussaint, A. (1984) *Virology* **137,** 102–112
39. Prentki, P., and Krisch, H. M. (1984) *Gene* (*Amst.*) **29,** 303–313
40. Ménard, R., Sansonetti, P., and Parsot, C. (1993) *J. Bacteriol.* **175,** 5899–5906
41. Bradford, M. M. (1976) *Anal. Biochem.* **72,** 248–254
42. Schägger, H., and von Jagow, G. (1991) *Anal. Biochem.* **199,** 223–231
43. Rauscher, L., Expert, D. Matzanke, B. F., and Trautwein, A. X. (2002) *J. Biol. Chem.* **277,** 2385–2395
44. Gardner, P. R. (2002) *Methods Enzymol.* **349,** 9–23
45. Varghese, S., Tang, Y., and Imlay, J. (2003) *J. Bacteriol.* **185,** 221–230
46. Moore, P. B., and Steitz, T. A. (2003) *Annu. Rev. Biochem.* **72,** 813–850
47. Lucas-Lenard, J., and Lipmann, F. (1971) *Annu. Rev. Biochem.* **40,** 409–448
48. Walker, C. A., Walsh, M. L., Pennica, D., Cohen, P. S., and Ennis, H. L. (1976) *Proc. Natl. Acad. Sci. U. S. A* **73,** 1126–1130
49. Zazialov, A. V., and Ehrenberg, M. (2003) *Cell* **114,** 113–122
50. Kreuzer, K. N., and Cozzarelli, N. R. (1979) *J. Bacteriol.* **140,** 424–435
51. Layer, G., Gaddam, S. A., Ayala-Castro, C. N, Ollagnier-de-Choudens, S., Lascou, D., Fontecave, M., and Outten, F. W. (2007) *J. Biol. Chem.* **282,** 13342–13350
52. Quail, M. A., Jordan, P., Grognan, J. M., Butt, J. N., Lutz, M., Thomson, A. J., Andrews, S. C., and Guest, J. R. (1996) *Biochem. Biophys. Res. Commun.* **229,** 635–642
53. Boyd, J. M., Pierik, A. J., Netz, D. J. A., Lill, R., and Downs, D. M. (2008) *Biochemistry* **47,** 8195–8202
54. Angelini, S., Gerez, C., Ollagnier-de Choudens, S., Sanakis, Y., Fontecave, M., Barras, F., and Py, B. (2008) *J. Biol. Chem.* **283,** 14084–14091
55. Gralnick, J. A., and Downs, D. M. (2003) *J. Biol. Chem.* **278,** 20708–20715
56. Pomposiello, P. J., Koutsolioutsou, A., Carrasco, D., and Demple, B. (2003) *J. Bacteriol.* **185,** 6624–6632
57. Skovran, E., Laubon, C. T., and Downs, D. M. (2004) *J. Bacteriol.* **186,** 7626–7634
58. Osborne, M. J., Siddiqui, N., Landgraf, D., Pomposiello, P. J., and Gehring, K. (2005) *Protein Sci.* **14,** 1673–1678
59. Justino, M. C., Almeida, C. C., Gonçalves, V. L., Teixeira, M., and Saraiva, L. M. (2006) *FEMS Microbiol. Lett.* **257,** 278–284
60. Justino, M. C., Almeida, C. C., Teixeira, M., and Saraiva, L. M. (2007) *J. Biol. Chem.* **282,** 10352–10359

# Siderophore-controlled Iron Assimilation in the Enterobacterium *Erwinia chrysanthemi* : EVIDENCE FOR THE INVOLVEMENT OF BACTERIOFERRITIN AND THE Suf IRON-SULFUR CLUSTER ASSEMBLY MACHINERY

Dominique Expert, Aïda Boughammoura and Thierry Franza

*J. Biol. Chem. 2008, 283:36564-36572.*
*doi: 10.1074/jbc.M807749200 originally published online November 6, 2008*

---